Integrated Fiber Optic Structural Health Sensors for Inflatable Space Habitats

Osgar John Ohanian III[*a], Naman Garg[a], Matthew A. Castellucci[a]

[a]Luna Innovations, Incorporated, Blacksburg, VA USA 24060

[*]ohanianj@lunainc.com, phone: 540-443-3872

ABSTRACT

Inflatable space habitats offer many advantages for future space missions; however, the long term integrity of these flexible structures is a major concern in harsh space environments. Structural Health Monitoring (SHM) of these structures is essential to ensure safe operation, provide early warnings of damage, and measure structural changes over long periods of time. To address this problem, the authors have integrated distributed fiber optic strain sensors to measure loading and to identify the occurrence and location of damage in the straps and webbing used in the structural restraint layer. The fiber optic sensors employed use Rayleigh backscatter combined with optical frequency domain reflectometry to enable measurement of strain every 0.65 mm (0.026 inches) along the sensor. The Kevlar woven straps that were tested exhibited large permanent deformation during initial cycling and continued to exhibit hysteresis thereafter, but there was a consistent linear relationship between the sensor's measurement and the actual strain applied. Damage was intentionally applied to a tensioned strap, and the distributed strain measurement clearly identified a change in the strain profile centered on the location of the damage. This change in structural health was identified at a loading that was less than half of the ultimate loading that caused a structural failure. This sensing technique will be used to enable integrated SHM sensors to detect loading and damage in future inflatable space habitat structures.

Keywords: Fiber optic, distributed strain sensing, structural health monitoring, inflatable space habitats, damage detection, webbing, woven straps.

1. INTRODUCTION

Multifunctional materials are desired as a solution to achieving weight savings for space applications while maximizing the utility of a structure. Weight is a key driving factor in the cost of space launch, especially for deep space missions. Inflatable space habitats are a viable approach to providing living quarters for humans in space, while reducing the weight and launch volume significantly. For instance, the Bigelow B330 module more than doubles the amount of living space per pound of structure when compared to the International Space Station (ISS) Destiny module[1]. While inflatable habitats hold promise for deep space missions, the structural integrity of these habitats over years of operation is a major concern. The lives of astronauts depend on the structural integrity; if the structure is damaged, an early warning system is needed to alert the crew. In addition, monitoring the structural integrity over long durations of time is also critical, since the flexible materials used to create inflatable habitats have been shown to exhibit creep [1][2] and other forms of degradation. Ongoing interest in monitoring and protection systems for space structures is evident from the literature [3][4]. New sensing technologies that can be integrated during the manufacturing process of thin ply composites and soft-goods materials are needed to enable structural health monitoring of inflatable space habitats.

To address these critical needs, high-definition distributed fiber optic sensing (HD-FOS) technology is employed to measure distributed strain and
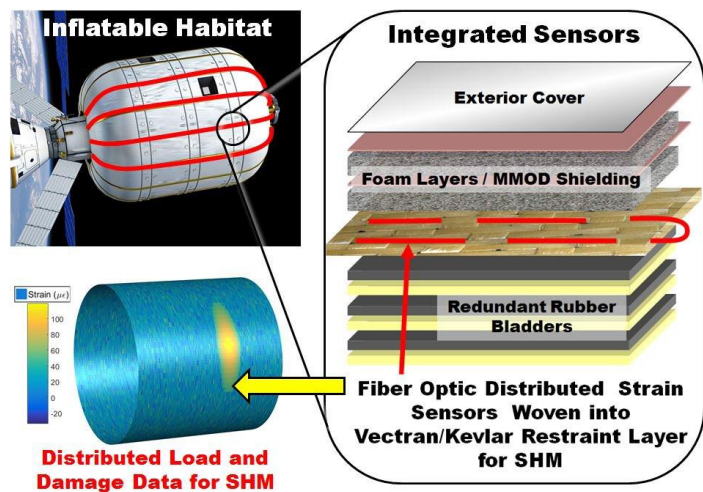

Figure 1: Integrated Fiber Optic SHM Sensors for Inflatable Space Habitat

---

[1] http://bigelowaerospace.com/b330/, retrieved 1/25/2016.

temperature in the webbing, cordage, and woven fabrics of the inflatable structures (Figure 1). The integrated sensors are intended to measure these quantities over many years. It is important to include thermal cycling measurement in interpreting the strain signals so that changes in strain patterns indicating degradation can be differentiated form normal deformations due to thermal expansion. The high spatial resolution of HD-FOS strain sensing will allow for identification of creep and stress concentrations indicative of future failure. The lightweight and flexible nature of the fiber optic sensors is compatible with the folding necessary for stowage during launch, and the sensors can be incorporated during the fabrication of inflatable structures rather than as a post process. This technology can provide unique high-resolution SHM data for inflatable space habitats that will be used in future space missions.

2. METHODOLOGY

Distributed strain measurements were used to visualize the changes in the state of flexible Kevlar straps. The strain profiles were correlated to overall loading and localized damage. The following subsections explain the technical approach employed.

2.1 Optical Frequency Domain Reflectometry

Optical frequency domain reflectometry (OFDR) allows thousands of sensing points with overlapping spectra in a single optical fiber to be read with sub-millimeter spatial resolution [5]. When interrogated by a laser light source, the Rayleigh backscatter of an optical fiber produces a random and stable spectral pattern, unique to each specific fiber, which is recorded by the instrument. Figure 2 (a) shows the reflected spectrum of a segment of Rayleigh backscatter from a piece of standard telecommunication-grade optical fiber (Corning SMF-28) [6]. Just as with a fiber Bragg grating (FBG), applied temperature or strain shifts the reflected spectrum of the scatter in the fiber at the location it is applied. Finding the frequency shift of the scatter spectrum is accomplished by performing a cross-correlation of the scatter spectrum from a measurement data set with that from a reference data set taken with the same fiber sensor in a known, nominal temperature or strain state. Figure 2 (b) shows the cross-correlation of a reference scatter spectrum with one that was perturbed by a temperature change. The correlation peak is shifted from center by a frequency shift resulting from the temperature change.
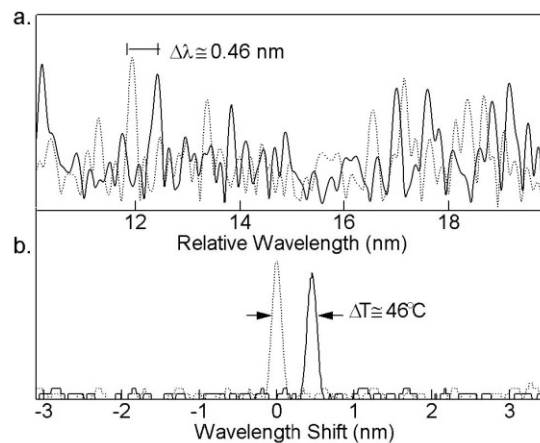

Figure 2: (a) Rayleigh scatter spectra along a 5 mm fiber segment for a heated (solid) and reference (dotted) scan. (b) Cross-correlation of the two spectra shows change in strain or temperature. [6]

When there is an induced strain, the frequency shift of the Rayleigh pattern relative to the reference state is calculated at every point along the length of the fiber. Distributed measurements of strain are made by first determining a gage length, which is typically on the order of a millimeter but can be larger or smaller. The average spectral shift for each gage length is determined. This shift is then converted to measured strain using known calibration coefficients appropriate to the fiber type. Using this procedure, detailed profiles of strain or temperature versus distance can be found along the entire length of the optical fiber. This technique has been successfully implemented for structural health monitoring by embedding fiber optic sensors in composite wind turbine blades [7].

2.2 Distributed Strain Measurement in Kevlar Straps

Distributed fiber optic sensors were bonded to flexible uncured Kevlar straps using a variety of adhesives. The basic design embedded the fiber optic sensor in a flexible polymer matrix that covered the Kevlar strap (Figure 3a). An incremental design iteration upon this successful design was to incorporate two passes of fiber in a single coated strap. The fiber termination and 180 degree turnaround were embedded in the coating to make the strap more rugged for handling, leaving only a single fiber lead and connector exiting the strap. This allowed for sensing directionality of damage (i.e. right side of the strap versus left), as well as the capability of sensing in-plane bending of the strap. Bending may occur if the weave pattern is shifted due to damage near the instrumented strap but not directly inflicted on it. A schematic of the final strap design is shown in Figure 3b.
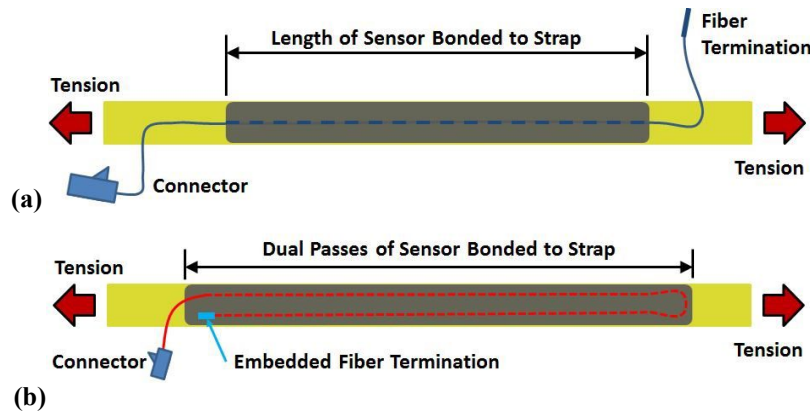

Figure 3: Fiber optic sensor embedded in flexible Kevlar strap, (a) Single pass sensor, (b) Dual pass fiber sensing strap.

Tension loading was applied to individual Kevlar straps using an ADMET load frame, pictured in Figure 4a. The distributed strain was measured using Luna's ODiSI-B (Figure 4b). Cyclic loading of the Kevlar straps was applied and the overall elongation was measured by the load frame and was compared to the distributed strain measurements.
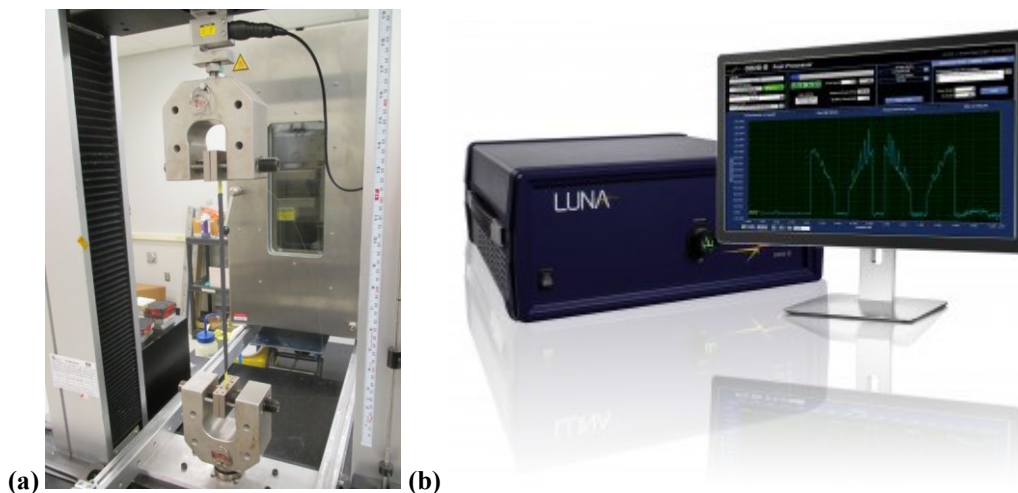

Figure 4: Test setup, (a) ADMET load frame for tensioning Kevlar straps with integrated fiber optic sensors, (b) ODiSI-B for distributed strain measurement.

2.3 Structural Health Monitoring of Inflatable Structure

Once the sensor integration technique was established, a subscale inflatable structure was fabricated to mimic the approach used in deployed inflatable space habitats. In this approach, a rubber bladder serves as the main pressure barrier, and is structurally supported by a woven network of Kevlar straps that form a restraint layer. The size of the straps was selected based on hoop stress calculations to mimic the same percentage of the maximum load rating that a full scale structure would experience. This resulted in a 12.7 mm (0.5 inch) wide Kevlar strap rated for 2.45 kN (550 lb) loading. Instrumented straps were incorporated in the structural restraint layer. The inflatable test article is shown in Figure 5.

Figure 5: Fabricated inflatable test article prototype, (left) Bladder bonded to endcaps, (center) Weaving process, (right) Finished inflatable structure, black straps are instrumented with fiber optic sensors.

There are two modes of measurement that are of interest for this kind of structure: load sensing, and damage sensing. The first test performed with the inflatable prototype was to determine if pressure loading could be reliably sensed. The experimental setup of the inflatable prototype is shown in Figure 6.
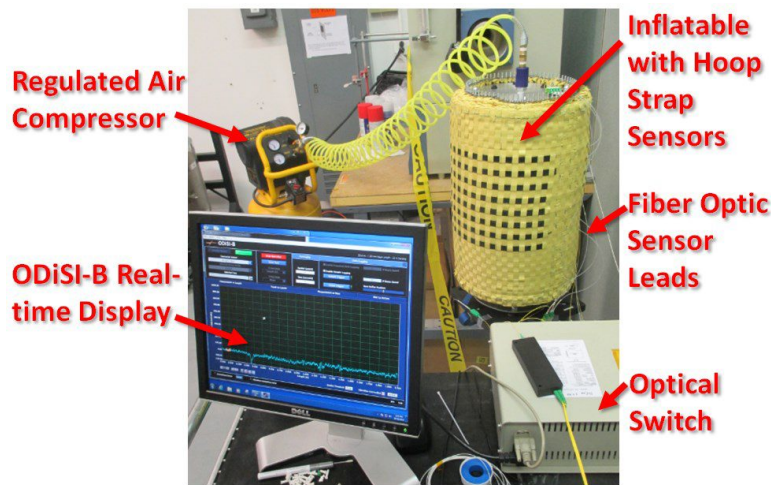

Figure 6: Experimental setup for SHM tests of inflatable prototype.

3. EXPERIMENTAL RESULTS

The following sections describe the experimental results from isolated strap tests as well as instrumented inflatable structure SHM tests.

3.1 Isolated Strap Test Results

Several rounds of testing were performed on isolated Kevlar straps to evaluate fiber optic integration techniques. In the final rounds of tests, the specimens were 12.7 mm (0.5 inch) wide Kevlar webbing rated for 2.46 kN (550 lb). Multiple loading cycles were performed to observe how the hysteresis of the strap changed over time. The results shown are for a case where cyclic loading was combined with intentional damage applied to the strap. The load vs displacement curves for three cycles are shown in Figure 7, with a cut in the strap applied in the second cycle at 0.44 kN (100 lb) loading, as shown in Figure 8.
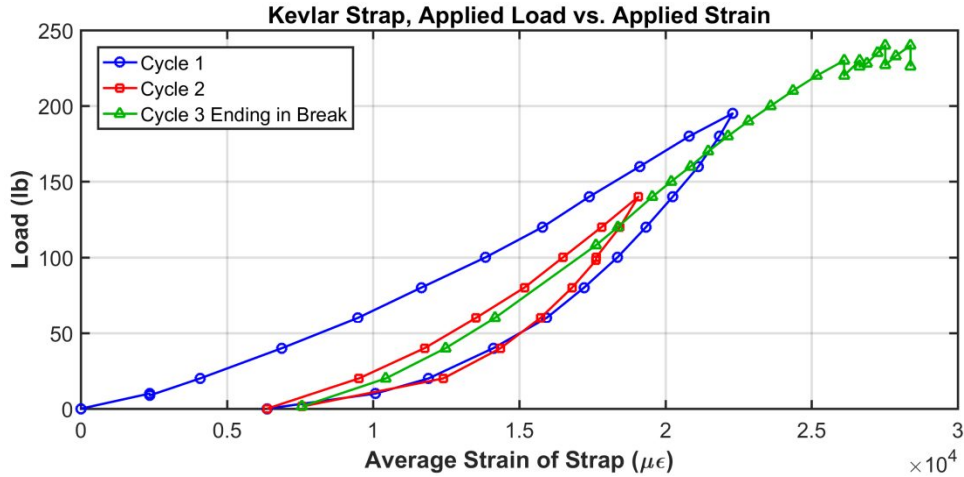
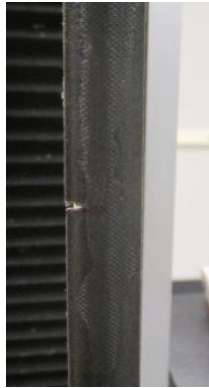Figure 7: Load vs displacement cycles of instrumented Kevlar strap.

Figure 8: Cut in Kevlar strap to determine if damage can be detected

The natural hysteresis of the Kevlar strap is evident in Figure 7; the average strain plotted is simply the elongation of the strap divided by the initial length. The cut in the strap was performed at 0.44 kN (100 lb) loading on the decreasing side of the second loading cycle. The change in trend at the end of the third cycle is due to the gradual failure of the strap ripping. The fiber optic distributed strain data along the length of the sensor is shown in Figure 9. The first cycle data shows the maximum strain of roughly 20,000 με applied with a 5,000 με residual (hysteresis) after unloading. The second cycle was re-baselined (tared) at 89 N (20 lb) loading, and shows a relative increase in strain of roughly 9,000 με and a smoother strain profile due to the subtraction of the residual strain. The middle section of each distributed strain measurement is relatively flat, with the edges gradually tending toward zero. This is attributed to the transition at the edge of the flexible bond of the sensing fiber experiencing no tension to full tension once the edge effects are passed. Depending on the bonding material, these edge effect regions can be abrupt or gradual. The most critical design goal was to demonstrate a uniform strain profile with efficient strain coupling between the sensor and the strap structural members over the middle region of the strap that was used for subsequent measurements.
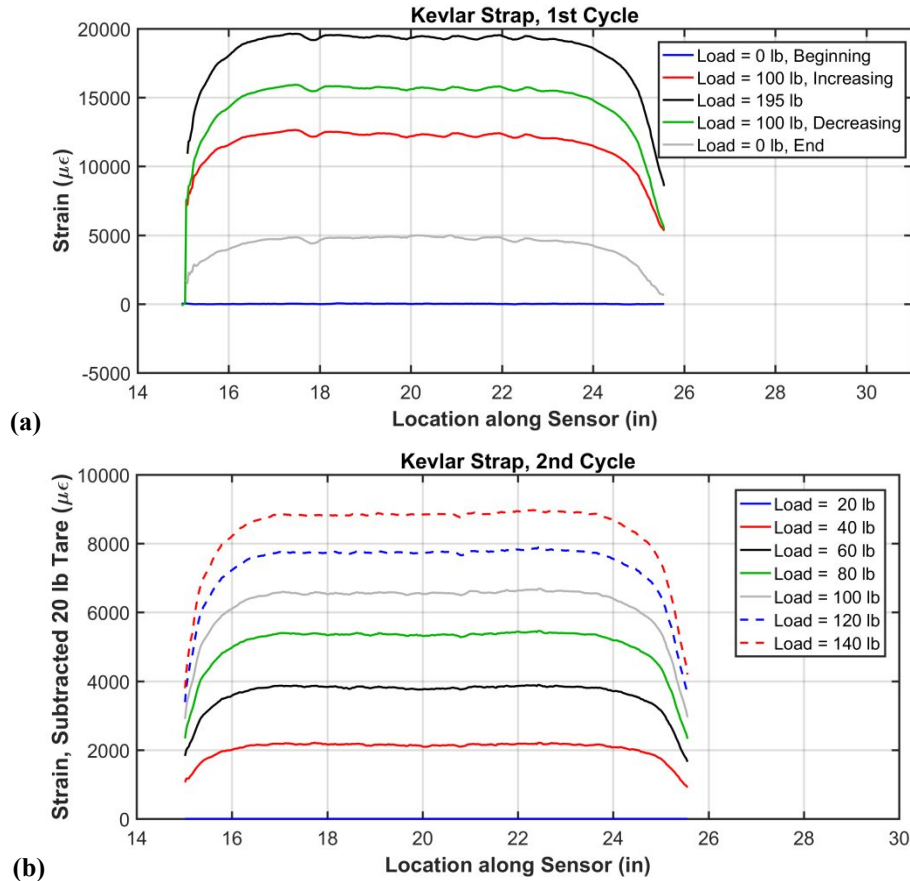
(a)

(b)

Figure 9: Strain profiles of instrumented strap, (a) Cycle 1 without tare (green and gray lines are on the decreasing leg of cycle), (b) Cycle 2 with tare at 89 N (20 lb) of loading subtracted.

While the Kevlar straps' strain response to loading is highly nonlinear, the sensor's measurement of strain is very linear with respect to the actual strain in the webbing, as seen in Figure 10. Even over several cycles with different hysteresis states, damage, and final breakage, the sensor output is relatively linear. The strain coupling for this sensor captured roughly 90% of the applied strain.
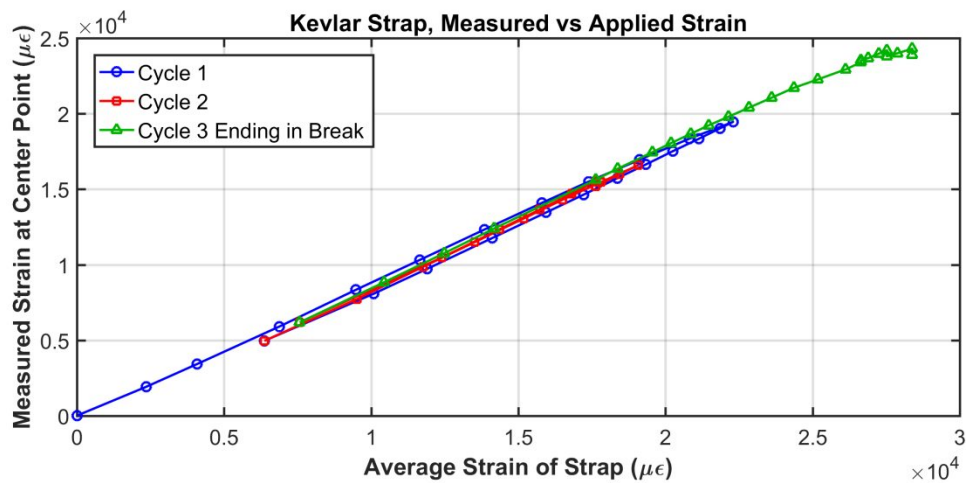

Figure 10: Cast urethane coated Kevlar strap measured strain vs applied average strain.

The next objective was to assess the damage sensing capability of the embedded sensor. When the cut was made, two immediate changes were observed. The loading on the strap decreased from 0.451 kN (101.5 lb) to 0.436 kN (98 lb); this was due to the control mode of the load frame maintaining displacement and letting load vary freely. In a real-world inflatable structure with constant internal pressure, this kind of failure would cause the strap to maintain the load and increase in strain. The second observation was that the shape of the strain profile being measured by the fiber optic distributed sensor changed. The data for this case are shown in Figure 11.
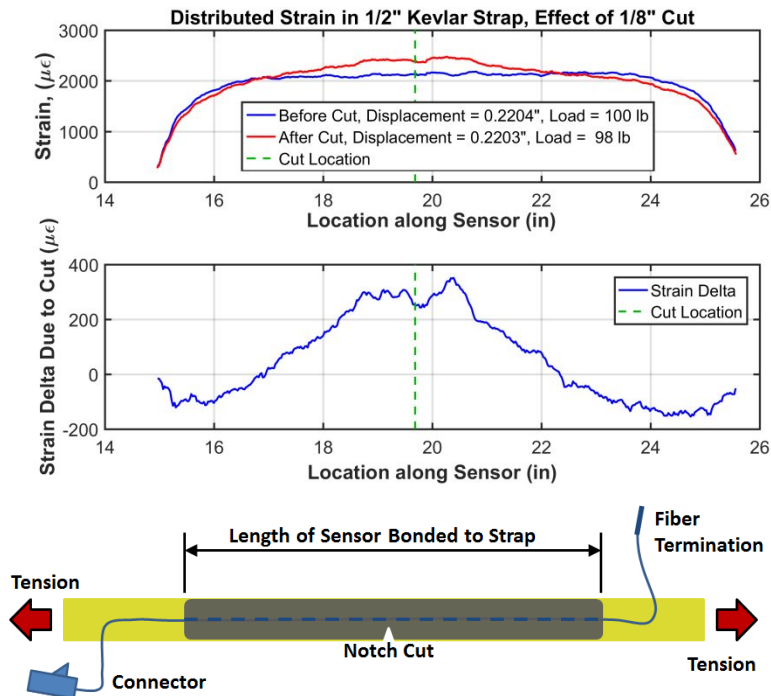

Figure 11: The effect of induced damage in Kevlar strap on distributed fiber optic strain measurement.

The top half of the plot in Figure 11 shows the relative strain profiles (with respect to a 0.356 kN / 80 lb loading case) before and after the induced damage. The green line shows the location of the cut on the strap in the sensor's coordinates. In general, the strain in the vicinity of the cut increases, while the edges of the strain profile decrease slightly in magnitude. This is much clearer in the bottom plot, where the difference between the before and after measurements is shown. There is a localized feature in the strain perfectly centered on the location of the cut. What was interesting and unexpected was how the effects are diffused over the entire strap. The decrease in strain at the two ends of the strap was unexpected, but this could possibly be explained by the fact that the load frame was maintaining displacement instead of tension. When the cut was made the load was forced to decrease. Because of the reduced cross-section of the strap at the cut, there was a localized increase in strain in that vicinity; however, the strap should slacken overall due to lower loading, and this was observed at the edges, furthest away from the cut. If loading were maintained rather than displacement, strain would remain constant at the edges (or possibly increase), with a larger increase in strain localized around the cut location.

In the next set of tests, the design improvement of including two passes of sensing fiber was evaluated for its damage sensing capabilities. The same experimental procedure was used as in the case of the single pass sensor tension test. At 0.445 kN (100 lbs) of tension a 1.6 mm (1/16") cut was applied to the top edge of the strap. The sensor on that side of the strap shows a localized strain increase, while the sensor on the bottom edge of the strap is unaffected. This can be seen in Figure 12b. When a larger cut is applied to the bottom edge at a different location along the strap, there is a noticeable localized strain increase observed in the bottom sensor with negligible effect on the top sensor within the strap (Figure 13). These results demonstrate two things: first, that damage as small as a 1.6 mm (1/16") tear in a 12.6 mm (1/2") strap is identifiable with this technique; second, that the location along the strap and directionality of which side of the strap was damaged can be clearly identified.
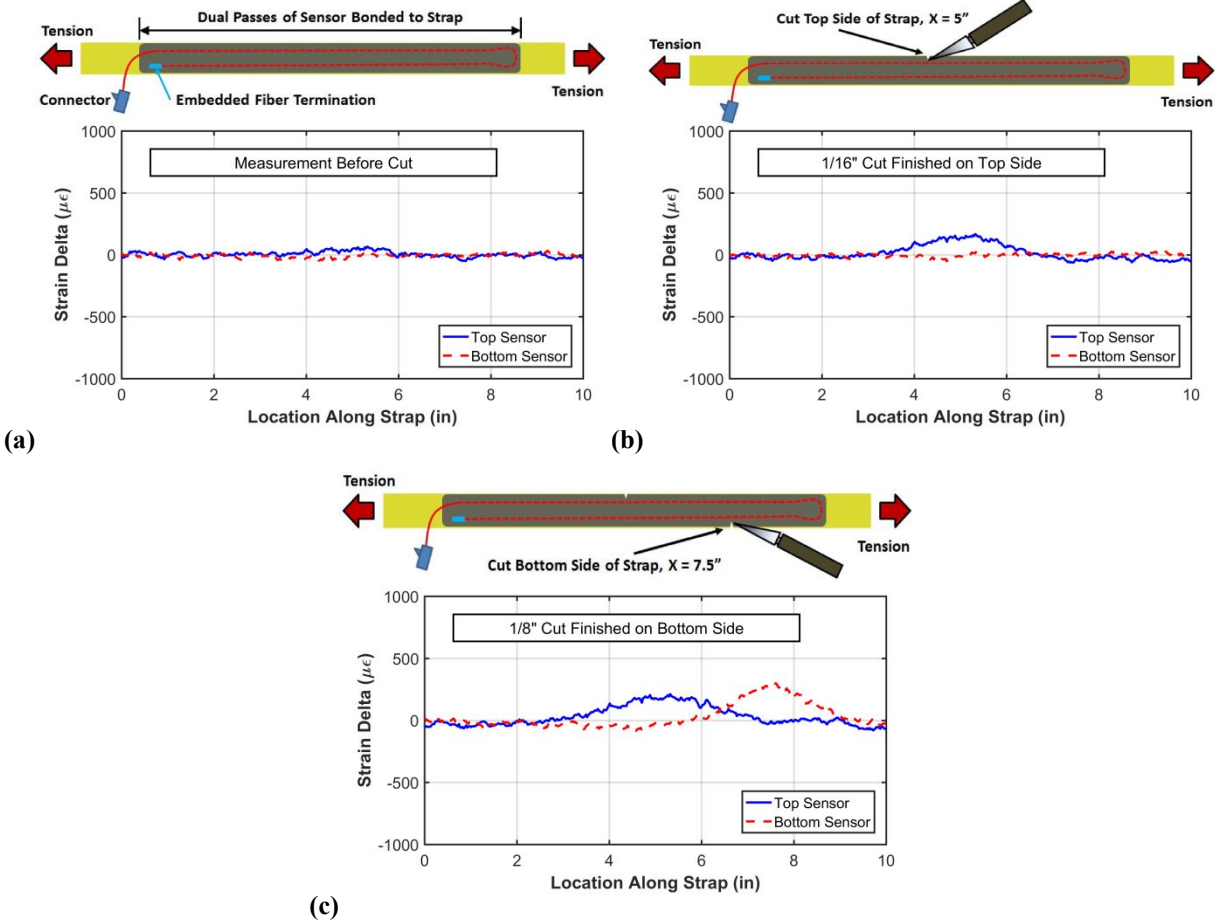
Figure 12: Dual pass sensor tension tests in ADMET load frame, (a) Initial state before cutting complete, (b) 1.6 mm / 1/16" cut on top edge of strap complete with top sensor clearly showing a localized strain increase, (c) 3.2 mm / 1/8" cut on bottom edge of strap with larger strain feature sensed by bottom sensor.

The next test performed with the dual pass sensing strap was to determine if bending motions could be identified in the sensor output. While the damaged strap was still under tension, the strap was pulled in the width-direction at the locations where the notch cuts had been applied. When the strap is bent towards the cut at x = 127 mm (5"), the top sensor is experiencing tension and the bottom sensor is experiencing compression, relative to the baseline state (0.445 kN / 100 lb of uniform tension). This phenomenon is clearly seen in the strain profiles shown in Figure 13. In addition, these dynamic movements of the strap and sensing of the bending loads did not alter the signature of the previous damage, which was still observable when the strap came to rest (Figure 13c). This is important because it demonstrates that the dual pass sensor strap can sense bending and damage independently, allowing for health measurements of the woven structure at a macro and micro level, respectively.
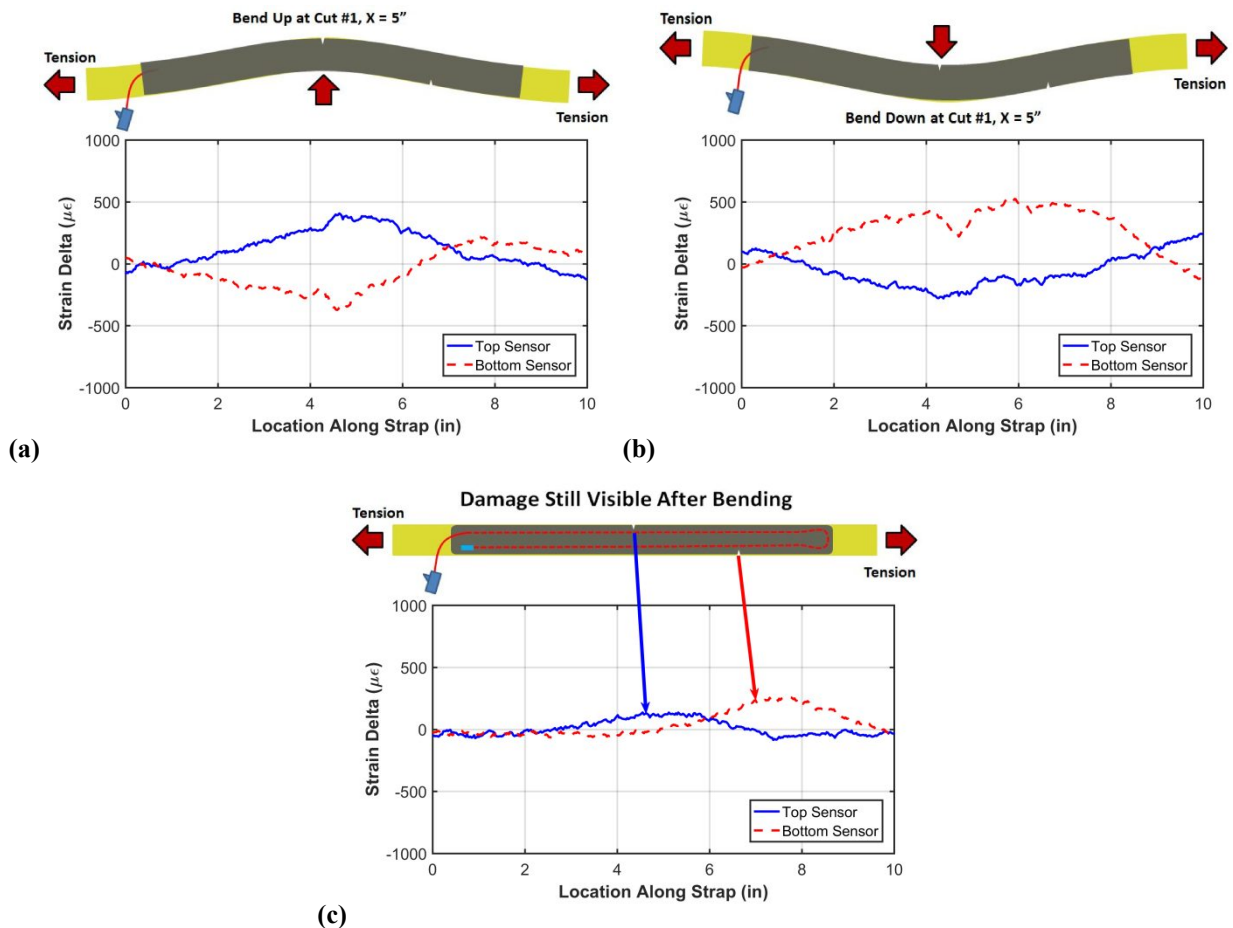
Figure 13: Dual pass sensor shows distinct pattern for in-plane bending, (a) Bending up, top sensor in tension, bottom sensor in compression, (b) Bending down, (c) Damage is still detectable after bending.

3.2 Inflatable Structure Test Results

Two sets of experiments were performed with the inflatable test specimen with integrated fiber optic sensors. First, a pressure loading test was performed. Then a set of induced damage tests were performed.

To assess pressure loading sensing, strain measurements were recorded at static pressure levels during inflation of the inflatable prototype. The baseline in the strain measurement was taken when the inflatable prototype was pressurized at 204.8 kPa (15 psig). Figure 14 shows the strain profile along the dual pass sensor on the hoop strap at increasing pressures. The location with near zero strain in the middle of the profile is where the fiber makes a 180 degree turn and there is a portion of the fiber not experiencing any axial strain. The strain profile remains consistent in shape as pressure is increased, as shown by the repeatability of the small strain variations that are seen along the strap. Strain was averaged over a 25.4 mm (1 inch) sub-section in the middle of the strap (from 30" to 31" from Figure 14) and plotted as a function of pressure in the bottom plot of Figure 14. The negative strain values from 184-198 kPa (12-14 psig) are a result of the 0με baseline taken at 204.8 kPa (15 psig). The correlation coefficient of 0.998 confirms a highly linear relationship between HD-FOS measured strain and inflation pressure in the prototype. This linearity between strain and pressure shows that distributed strain measurements will be consistent under pressure changing conditions when a baseline is taken after inflation. The positive results from this test are important because they show that HD-FOS can be used to measure loading of the straps in the restraint layer, and calibrated to measure system pressure with the ability to detect a systemic loss in pressure that may indicate a structural failure or leak.
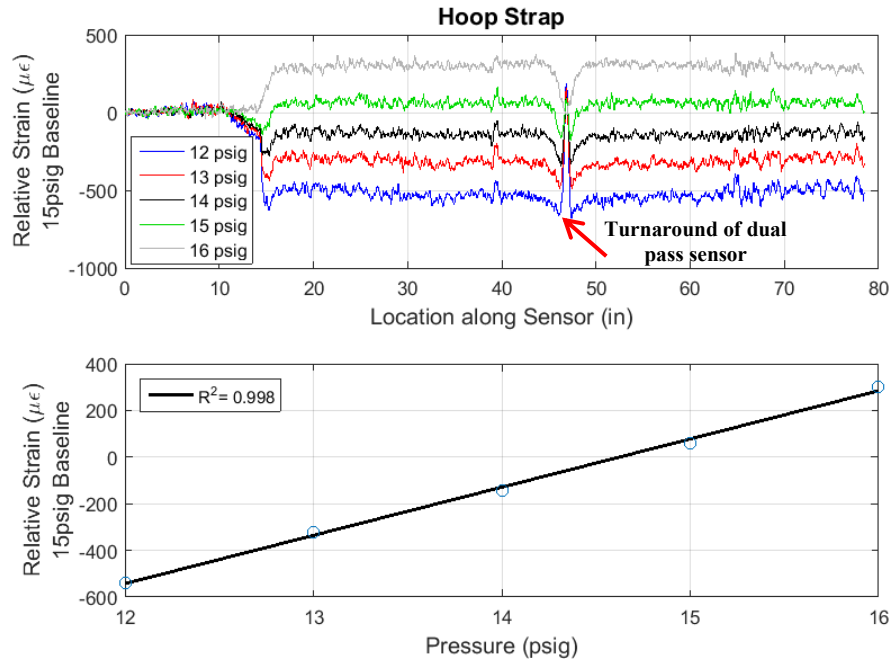
Figure 14: Inflatable prototype pressure loading test with the baseline strain taken at 204.8 kPa / 15 psig, (top) Strain profile along the dual pass sensor on the hoop strap at increasing pressures, (bottom) Linear relationship between strain in strap and pressure.

The final tests were intended to sense damage inflicted on sub-scale inflatable structure. The structure incorporated eight hoop straps with integrated dual pass fiber optic sensors. Each strap was calibrated and re-baselined at the nominal inflation load of 204.8 kPa (15 psig), to allow for observation of changes in strain at this condition. It is estimated that at 204.8 kPa (15 psig) the tension in the straps is in the vicinity of 178 to 222 N (40 to 50 lb), which is less than the load frame tests of isolated straps. The first SHM test involved cutting a notch in one of the sensing hoop straps. The cut was performed using Kevlar shears, and the cut was measured as 1.63 mm (0.064") out of the full strap width of 12.6 mm (0.50"), as seen in Figure 15a & b. The corresponding strain measurement shows (Figure 15c) a clear peak on the bottom sensor and a smaller peak in the top sensor. This strain feature is much sharper than the isolated strap tests; it is hypothesized that since the straps are woven together in a plain weave, the friction between straps limits how far the strain can be distributed when damage occurs, and consequently produces a larger localized peak.

This test demonstrates the ability to sense which side of the restraint strap has been damaged. In this inflatable test, the strain increase is narrower in location and higher in magnitude than the individual strap tests performed in the ADMET load frame. There are several possible explanations for this: first, the weave pattern may isolate sections of the strap to shorter increments where strain can be more severe due to damage; second, bulging of the bladder during an inflatable test could not be simulated on the linear load frame; and third, the load frame maintained displacement rather than load while the pressure will conversely maintain loading and increase the strain. Overall, the sensing technique appears to be more sensitive for the target application than in the preliminary simulated conditions.
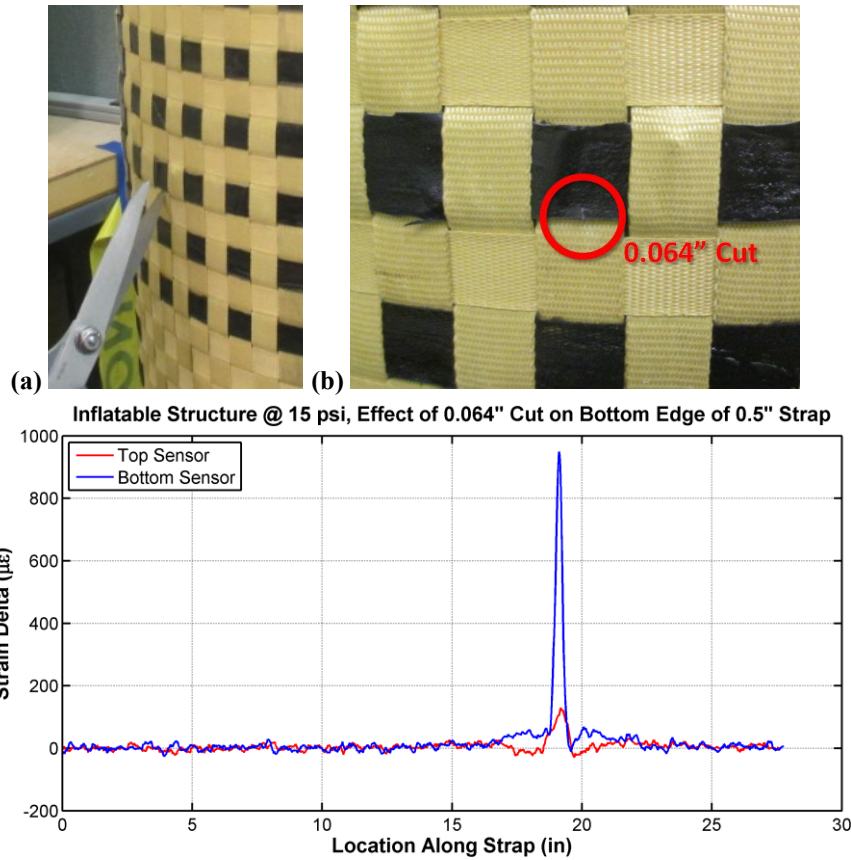
Figure 15: Effect of damage inflicted on dual pass sensing strap in inflatable prototype at 204.8 kPa / 15 psig, (a) Cutting strap with Kevlar shears, (b) 1.26 mm / 0.064" cut on Hoop Sensor 3, (c) Localized strain peak at location of cut, bottom sensor shows much larger response because cut was applied to bottom edge of strap.

The next objective was to determine if the sensing straps could detect damage in adjacent straps that were not instrumented with sensors. A 1.52 mm (0.060") cut was applied to a non-instrumented strap as seen in Figure 16a. There is an observable change in the sensing strap near the damage, as can be seen in Figure 16b, but it is of a different nature than the previous result where the sensing strap was directly damaged. In this case, the effect on strain is spread much wider along the length of the strap (245 mm / 10 inches versus 24.5 mm / 1 inch in the previous case) and is lower magnitude (175 $\mu\epsilon$ versus 1000 $\mu\epsilon$ in the previous case). In addition, there is an oscillatory characteristic to this strain measurement that can be attributed to the period of the weave pattern where the instrumented hoop strap must go over and under axial straps. These differences in strain measurement demonstrate that the type of damage may be able to be determined based on the shape of the strain profile measured during an SHM measurement.
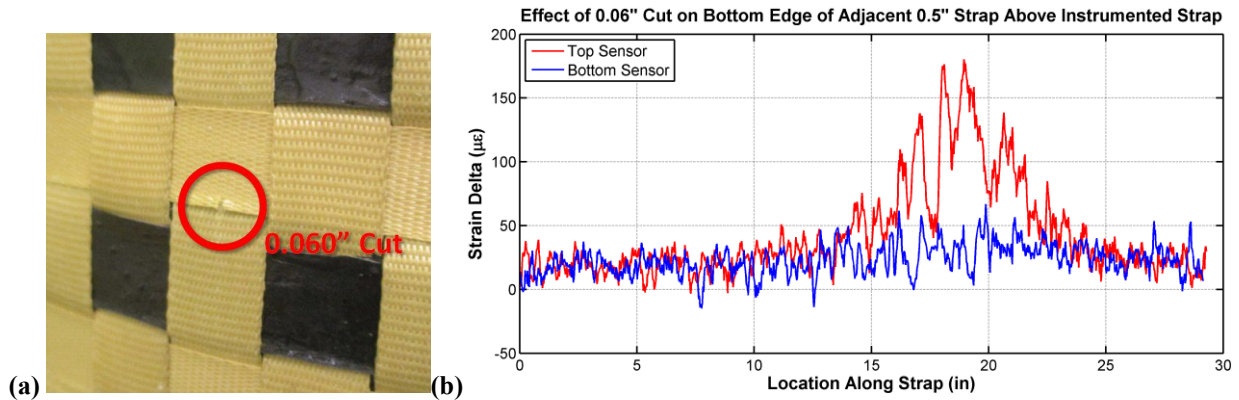
Figure 16: Damage inflicted on non-instrumented adjacent strap in inflatable prototype at 204.8 kPa / 15 psig, (a) 1.52 mm / 0.060" cut applied to bottom edge of Kevlar strap, (b) Strain measurement in sensor strap below cut location.

The next test was performed to determine if the magnitude of the damage to a sensing strap could be reliably detected. To accomplish this, multiple successively deeper cuts were applied to one location of a dual pass sensing strap. The results are shown in Figure 17. Damage was sensed from cuts as small as 0.76 mm (0.030"). In addition, the magnitude of the change in strain due to successive cuts grew with each increase in damage. The bottom sensor within the strap correctly showed larger strain response to the cut that was applied to that side of the strap. These results give confidence that the fiber optic SHM technique should be able to localize damage and estimate the extent of damage to inflatable restraint layers to assess the overall health of the structure.
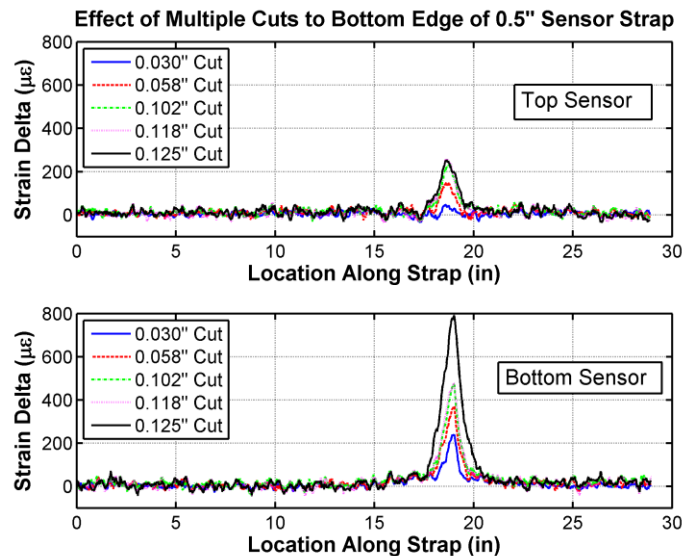

Figure 17: Sensing of repeated damage events.

One final test was performed with the inflatable prototype to demonstrate that a previously damaged sensing strap could also successfully sense damage in an adjacent strap at a later time. A new cut was applied to the non-instrumented strap above the previously damaged strap with cuts of increasing depth, but this time at a different location along the hoop strap. The cut was intended to be on the order of 3 mm (0.12") but ended up larger than expected, cutting 6.4 mm (0.25") of the overall width of the 12.6 mm (0.5") strap. Bulging of the rubber bladder in the vicinity of the cut was observable, and this was by far the largest amount of damage tested with this structure. A photograph of the cut and a plot of the resulting strain measurement are seen in Figure 18. The strain measurement shows a large magnitude and widely affected section of the sensing strap due to the cut in the adjacent strap. It should be noted that there was still a peak in strain at the location of the previous damage to the sensing strap superimposed with the strain increase due to the adjacent strap being partially severed. This is an important result because it shows that partial damage to a sensing strap

does not render it useless, but rather it can still sense changes in the structural health over time and spanning the full extent of the strap's length.
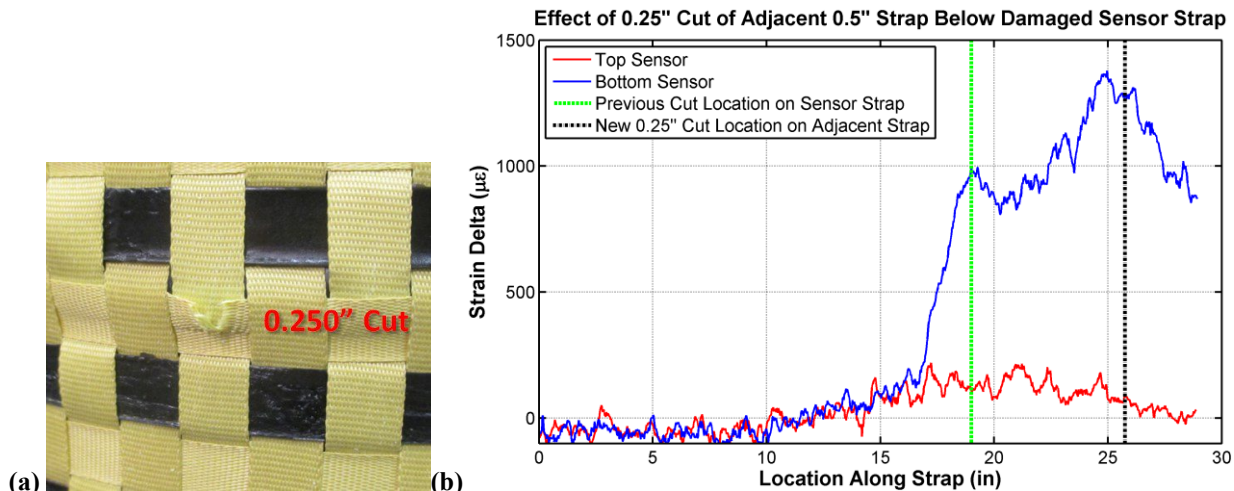

Figure 18: Sensing damage in adjacent straps after sensor strap has sustained damaged, (a) Large cut to adjacent strap causing deformation of weave pattern and bulge in bladder, (b) Large and wide strain signal due to 6.3 mm / 0.25" cut, while a strain peak still exists where the sensing strap was previously damaged.

4. CONCLUSIONS

This research has explored and proven the feasibility of using Rayleigh-based optical frequency domain reflectometry (OFDR) distributed fiber optic strain measurements to quantify loading and detect damage in flexible Kevlar straps. This is an important finding that can enable structural health monitoring of inflatable structures, such as space habitats. The 0.65 mm (0.026 inch) spacing between strain measurements along the embedded sensing fiber provided excellent resolution to observe changes in the state of the structure. While the instrumented Kevlar straps exhibited large nonlinear hysteresis during cyclic loading, the integrated fiber optic sensors maintained a linear relationship between measurements and the actual strain. A Kevlar strap with dual passes of a single sensing fiber was able to detect in-plane bending of the strap. The final set of experiments was performed with an inflatable test specimen that incorporated fiber optic sensors in the straps of the restraint layer. Inflation pressure was correlated with the distributed strain measurements with excellent linearity. The inflatable structure was then intentionally damaged to determine if the sensors could detect this change is structural health. The integrated sensors were able to identify and localize the occurrence of damage in instrumented straps as well as adjacent non-instrumented straps. These findings demonstrate the potential of the HD-FOS technology to play a critical role in structural health monitoring of future inflatable space habitats.

5. ACKNOWLEDGEMENTS

REFERENCES

[1] Selig, M. M., Valle, G. D., James, G. H., Oliveras, O. M., Jones, T. C., Doggett, W. R., "Creep Burst Testing of a Woven Inflatable Module," Proc. 2nd AIAA Spacecraft Structures Conference, (2015).
[2] Kenner, W. S., Jones, T. C., Doggett, W. R., Duncan, Q., Plant, J., "Environmental Effects on Long Term Displacement Data of Woven Fabric Webbings Under Constant Load for Inflatable Structures," Proc. 56th AIAA/ASCE/AHS/ASC Structures, Structural Dynamics, and Materials Conference, (2015).
[3] Studor, G., "Lessons Learned JSC Micro-Wireless Instrumentation Systems on Space Shuttle and International Space Station" presented at the CANEUS, Grapevine, Texas, (2006).

[4] Christiansen, E. L., "Handbook for Designing MMOD Protection," NASA Johnson Space Center, TM-2009-214785, (2009).

[5] Duncan, R., Childers, B., Gifford, D., Petit, D., Hickson, A., Jackson, A., Duke, J., Brown, T., "Use of a Fiber-Optic Distributed Sensing System for Nondestructive testing of Aerospace Structures," *Materials Evaluation* 61, 838 (2003).

[6] Kreger, S. T., Gifford, D. K., Froggatt, M. E., Soller, B. J., & Wolfe, M. S., "High resolution distributed strain or temperature measurements in single-and multi-mode fiber using swept-wavelength interferometry". In Optical Fiber Sensors p. ThE42 (2006).

[7] Pedrazzani, J.R., Klute, S. M., Gifford, D. K., Sang, A. K., and Froggatt, M. K., "Embedded and surface mounted fiber optic sensors detect manufacturing defects and accumulated damage as a wind turbine blade is cycled to failure," Proc. 2012 SAMPE Technical Conference, Baltimore, MD, May 21-24, (2012).